R. & M. No. 3002
(17,230)
A.R.C. Technical Report

MINISTRY OF SUPPLY

AERONAUTICAL RESEARCH COUNCIL
REPORTS AND MEMORANDA

Flow in the Laminar Boundary Layer near Separation

By

B. S. STRATFORD, Ph.D.
With an Appendix by Dr. G. E. GADD, of the Aerodynamics Division, N.P.L.

LONDON: HER MAJESTY'S STATIONERY OFFICE
1957
EIGHT SHILLINGS NET

Flow in the Laminar Boundary Layer near Separation

By

B. S. STRATFORD, Ph.D.

COMMUNICATED BY PROFESSOR H. B. SQUIRE

With an Appendix by DR. G. E. GADD, of the Aerodynamics Division, N.P.L.

Reports and Memoranda No. 3002

November, 1954

Summary.—A simple formula is derived for the separation of the laminar boundary layer. The method of derivation and a key test suggest that it should be reasonably accurate and of general application, including particularly the range of sharp pressure gradients and small pressure rises to separation.

In addition a partially new exact solution is found for the boundary-layer equations of motion; also the pressure distribution is obtained for continuously zero skin friction, this pressure distribution being expected to attain any given pressure rise in the shortest distance possible for a given laminar boundary layer provided that there is neither transition nor boundary-layer control.

The final formula of the paper is given by equation (41); equation (43) is a simpler but rather less accurate formula. The pressure distribution for continuously zero skin friction is represented by equation (39) and is shown in Fig. 3 as curve (c).

Preface.—This paper is an abridged version of a thesis approved for the degree of Doctor of Philosophy in the University of London.

1. *Introduction.*—With so many methods already existing for the prediction of laminar boundary-layer separation, as for example in Refs. 1 to 7, some apology is perhaps needed for the introduction of yet another. There does however still seem to be some requirement for a method that combines, together with a reasonable combination of simplicity and accuracy, a direct and intuitively helpful analysis of the flow. In particular this is true for application to small sharp pressure rises, where many existing methods fail. The present method aims at satisfying this requirement; it also considers the flow where the boundary layer is continuously on the point of separation, this flow attaining any given pressure rise in the shortest distance possible for a given initial boundary layer.

In the course of the analysis a new exact solution is discovered for a flow closely related to laminar boundary-layer flow.

2. *Physical Derivation* (*see Figs. 1 and 2 for a Summary of the Treatment*).—2.1. *The Outer Layer.*—Consider the flow in a boundary layer for which the pressure is constant between $x = 0$ and $x = x_0$ and for which an arbitrary pressure rise starts at $x = x_0$, as in Fig. 1.

Suppose first of all that the outer part of the boundary layer were to become inviscid for $x > x_0$, so that the total head along a streamline in this region remained constant. Then the solution for the velocity profile would be

$$(\tfrac{1}{2}\rho u^2)_{(x,\psi)} \equiv [(\tfrac{1}{2}\rho u^2)_{(x_0,\psi)} - (p - p_0)] \text{ if } \mu = 0 \text{ for } x > x_0, y > \delta_s \quad \ldots \qquad (1a)$$

where $\psi = \int_0^y u\, dy$, where the suffix ψ on each side of the equation implies that all terms refer to the same streamline, and where $y > \delta_s$ limits the whole application to the outer part of the boundary layer.

To this partially inviscid solution has to be added an increment due to the effect of viscosity between positions x_0 and x.

Now the shape of the velocity profile in the outer part of the boundary layer is not greatly affected by a pressure rise, provided this is small, despite the change in the general level of velocity; consequently the viscous forces on any fluid element are the same to first-order accuracy as if there were no pressure rise. But for no pressure rise the increment from viscosity between positions x_0 and x is just

$$[(\tfrac{1}{2}\rho u_b^2)_{(x,\psi)} - (\tfrac{1}{2}\rho u_b^2)_{(x_0,\psi)}]$$

where u_b is the Blasius flat-plate solution. Superposing this increment on the solution (1a) gives

$$(\tfrac{1}{2}\rho u^2)_{(x,\psi)} \equiv [(\tfrac{1}{2}\rho u_b^2)_{(x,\psi)} - (p - p_0)] \text{ for } y > \delta_s\,, \qquad \text{(1b)}$$

the essential change between equations (1a) and (1b) being the reference in equation (1b) to the corresponding Blasius flow u_b at x instead of to the original flow at x_0.

With qualifications, equation (1b) represents a 'general' solution for the flow in the outer boundary layer. The first equation, *i.e.*, (1a), is exact when the viscosity is zero in the outer layer downstream of x_0; equation (1b) is a closer approximation evolved from it in order to allow for the omitted region of viscosity. The superposition of viscous and pressure effects in this manner is asymptotically accurate only for short sharp pressure rises, but it is a vital step in the physical derivation and provides a basis for convenient empirical extension to larger pressure rises. The solution (1b) may be restated:

(Dynamic head at any point along a given initial streamline) = (Dynamic head at the same distance downstream along the same initial streamline, were there viscosity—but no pressure changes) − (The increment of dynamic head that would be converted to static pressure, were there the actual pressure changes—but no viscosity) .

The utilitarian advantage of this as a statement of superposition is of course that it enables the use in combination of two exact solutions, or integrations, of the boundary-layer equations of motion, *i.e.*, the Blasius solution for zero pressure change, and the Bernoulli equation for zero viscosity. No intermediate step-by-step numerical work is required and results can be obtained directly and explicitly at any position x.

The above can readily be confirmed algebraically by expressing the boundary-layer equation of motion as

$$\frac{\partial}{\partial s}(p + \tfrac{1}{2}\rho u^2) = \mu \frac{\partial^2 u}{\partial y^2}\,, \qquad \text{(2)}$$

and then considering the first two terms in the Taylor expansion:

$$(p + \tfrac{1}{2}\rho u^2)_{(x,\psi)} \equiv (p + \tfrac{1}{2}\rho u^2)_{(x_0,\psi)} + \left[\frac{\partial}{\partial s}(p + \tfrac{1}{2}\rho u^2)\right]_{(x_0,\psi)} (x - x_0) + \ldots\ldots \qquad \text{(3)}$$

The first term on the right-hand side is independent of the pressure rise as the singularity at $x = x_0$ is confined to $y = 0$, and similarly for the second term as substitution from equation (2) gives it to be equal to $\mu(\partial^2 u/\partial y^2)_{(x_0,\psi)}(x - x_0)$. Hence the left-hand side is the same as if the pressure rise were zero, *i.e.*,

$$(p + \tfrac{1}{2}\rho u^2)_{(x,\psi)} \equiv (p_b + \tfrac{1}{2}\rho u_b^2)_{(x,\psi)} \qquad \text{(4)}$$

provided higher terms may be neglected, and this equation represents the superposition result of equation (1b).

Extension of the same arguments gives the corresponding identities

$$\left(\frac{\partial u}{\partial y}\right)_{(x,\psi)} = \left(\frac{\partial u_b}{\partial y}\right)_{(x,\psi)} \qquad \text{(5)}$$

and

$$\left(\frac{1}{u}\frac{\partial^2 u}{\partial y^2}\right)_{(x,\psi)} = \left(\frac{1}{u_b}\frac{\partial^2 u_b}{\partial y^2}\right)_{(x,\psi)}\,, \qquad \text{(6)}$$

the order of accuracy of equation (6), as far as it affects the present method, being equivalent to that of the earlier equations.

2.2. *The Sub-layer.*—The above solution for the outer layer, by means of a principle of superposition, is in contrast to the situation in the region very close to the wall—here called the sub-layer. At all stations x the dynamic head is zero at the wall. Thus the inertia forces are zero and the pressure gradient force must be balanced entirely by the viscous force, *i.e.*,

$$\mu \left(\frac{\partial^2 u}{\partial y^2}\right)_{y=0} = \frac{\partial p}{\partial x} \qquad \text{(7)}$$

which is also a standard boundary condition from the equations of motion. But at separation

$$\left(\frac{\partial u}{\partial y}\right)_{y=0,\, x=x_{\text{sep}}} = 0\,. \qquad \text{(8)}$$

Further examination of the wall boundary conditions indicates that if $\partial^2 p/\partial x^2 = 0$*,

$$\left.\begin{aligned} &\frac{\partial^3 u}{\partial y^3} = 0\,, \\ \text{but} \quad &\frac{\partial^4 u}{\partial y^4} \neq 0 \end{aligned}\right\} \text{at } y = 0 \qquad \text{(9)}$$

(Ref. 8 shows that these hold at separation despite the singularity), while if $(\partial u/\partial y)_{y=0} \equiv 0$ at all x, a concept for which reference may be made to Falkner and Skan's well known solutions,

$$\left.\begin{aligned} &\frac{\partial^3 u}{\partial y^3} = 0\,, \quad \frac{\partial^4 u}{\partial y^4} = 0\,, \quad \frac{\partial^5 u}{\partial^5 y} = 0\,, \\ \text{but} \quad &\frac{\partial^6 u}{\partial y^6} \neq 0 \end{aligned}\right\} \text{at } y = 0\,. \qquad \text{(10)}$$

These being exact conditions, it follows that a good ' fit ' to the velocity profile close to the wall when $x = x_{\text{sep}}$ and $\partial^2 p/\partial x^2 = 0$ is given by formally putting

$$u = \frac{y^2}{2!} \cdot \frac{1}{\mu} \frac{\partial p}{\partial x} + \frac{y^4}{4!} \cdot h \qquad \text{(11)}$$

provided h, considered as a disposable parameter, is given an appropriate value. Likewise,

$$u = \frac{y^2}{2!} \cdot \frac{1}{\mu} \frac{\partial p}{\partial x} + \frac{y^6}{6!} \cdot j \qquad \text{(12)}$$

is a good fit when $\partial^2 p/\partial x^2$ is such that $(\partial u/\partial y)_{y=0}$ is continuously zero for all x. This procedure is analogous to the Pohlhausen method. In the present application however it is applied only to the sub-layer (roughly the part inside the point of inflexion) this having a simpler shape than the whole profile and one that can be fitted quite accurately. A further difference from the Pohlhausen method is that the type of curve used is varied according to the value of the higher derivative $\partial^2 p/\partial x^2$ in order to satisfy more boundary conditions and obtain a closer representation of the profile.

It will be noticed that this solution for the sub-layer is controlled largely by the value of $\partial p/\partial x$ at the local position x, i.e., the sub-layer is not a ' historic ' region in the sense of being determined from its own sub-layer profiles upstream. This is because the sub-layer is a region of ' viscous control ', the inertia forces being very small and the profile being able, and in fact being forced, first to fit at the join with the outer layer—to this extent it is historic as the outer layer is historic—and then to adjust itself so that the viscous forces balance most of the force from the local pressure gradient.

All that now remains is to join these two parts of the profile, but before doing so it is worthwhile to examine briefly both the development of these two regions and the transition between them.

* Equation (9) applies more generally than to $\partial^2 p/\partial x^2 = 0$. The single condition for $\partial^2 p/\partial x^2$, however, is chosen in order to correspond with the mathematical derivation of section 3.

2.3. *A Picture of the Flow.*—When the sudden pressure gradient is applied at $x = x_0$, conditions at $y = 0$, $x = x_0$ must change discontinuously in order that the boundary conditions $\mu(\partial^2 u/\partial y^2) = \partial p/\partial x$ may still hold. This point region here corresponds to the sub-layer. Other than at $y = 0$, however, the only effect of the pressure gradient at $x = x_0$ is to start to reduce the dynamic head almost independently along each streamline, hence the principle of superposition in the outer layer. At positions downstream of x_0 the influence of the singularity has spread from $y = 0$, and the sub-layer corresponds roughly to the region inside the point of inflexion of the velocity profile. The limit of the sub-layer at any station x is readily obtained by an extension of the present method, its limit being effectively finite, as assumed here, just as for an ordinary boundary layer (strictly, however, both layers only gradually merge into the external flow, there being no definite joining point). Only at $y = 0$ in the sub-layer does the viscous force exactly balance the pressure gradient, while at the join with the outer layer the flow fully satisfies the outer-layer conditions; the region between these two points, *i.e.*, the whole of the sub-layer other than for its boundaries, is a region of transition. This transition is brought about, algebraically, by the higher terms shown in the Taylor expansion for the sub-layer, these reducing the value of $\partial^2 u/\partial y^2$ from a maximum at the wall to zero at the point of inflexion. Physically, the transition is between a balancing of the pressure gradient by viscous forces and a balancing of it by inertia forces.

2.4. *The Joining Condition and the Final Results.*—For joining the sub-layer and outer-layer continuity is postulated in ψ, u, $\partial u/\partial y$, and $\partial^2 u/\partial y^2$. It is important to include ψ of course, it being well known for example that small amounts of boundary-layer suction can significantly affect separation. These four boundary conditions on the sub-layer are sufficient to finalize the profile and to show that the position of separation must satisfy

$$\left[C_p \left(x \frac{\partial C_p}{\partial x}\right)^2\right] = 6 \cdot 48 \times 10^{-3} \text{ when } \frac{\partial^2 p}{\partial x^2} = 0 \quad .. \quad .. \quad .. \quad .. \quad (13)$$

where C_p is the pressure coefficient $\dfrac{p_{\text{sep}} - p_0}{\frac{1}{2}\rho U_0^2}$,

or, $$\left[C_p \left(x \frac{\partial C_p}{\partial x}\right)^2\right] = 4 \cdot 92 \times 10^{-3} \quad .. \quad .. \quad .. \quad .. \quad .. \quad .. \quad (14)$$

when $\partial^2 p/\partial x^2$ is such that $(\partial u/\partial y)_{y=0} \equiv 0$ for all $x > x_0$. It will be noted that the difference in $\partial^2 p/\partial x^2$ changes only the value of the numerical constant, as between $6 \cdot 48 \times 10^{-3}$ and $4 \cdot 92 \times 10^{-3}$.

The above results, *i.e.*, equations (13) and (14), will determine the position of separation for a given pressure distribution provided the value of $\partial^2 p/\partial x^2$ is appropriate to the value of the numerical coefficient employed and provided the distance to separation is small enough for the derivation to remain valid..

The physical derivation that has just been given is summarized in Figs. 1 and 2, where suffix $_a$ is used to denote the flow with pressure gradient.

The results of the physical derivation will be generalized and made more accurate in the next section by exact fitting at four positions in the double-parameter field represented by $(\partial^2 p/\partial x^2)_{x_{\text{sep}}}$ and $(x_{\text{sep}} - x_0)$.

As an extension of the above, integration of the differential equation (14), which must hold at all points $x > x_0$, yields the pressure distribution for continuously zero skin friction:

$$C_{p,\,\tau_0 \equiv 0} = 0 \cdot 223 \left\{\log \frac{x}{x_0}\right\}^{2/3} . \quad .. \quad .. \quad .. \quad .. \quad .. \quad (14a)$$

This pressure distribution is almost identical with that shown in Fig. 3 as curve (b). Its possible practical significance is that, for a given initial boundary layer, and given neither boundary-layer control nor transition, flow with continuously zero skin friction (*i.e.*, flow which is always just at the point of separation) can be shown to attain any required pressure rise almost certainly in the shortest posssible distance, and with the minimum growth of boundary layer. Hence, on say an aerofoil, it causes the minimum possible dissipation of energy and the minimum possible increment of drag for the postulated conditions. This type of flow receives further consideration in the mathematical derivation.

3. *Mathematical Derivation.*—The mathematical derivation considers in more detail and by more exact methods the types of flow upon which the physical method has focussed attention. The results from the physical derivation are first rederived in a nominally exact form, and are then extended empirically to cover a wider range of types of pressure distribution.

The physical approach of the previous section has given a solution which applies to the limited field of small values of $(x_{sep} - x_0)$, for two particular values of $(\partial^2 p/\partial x^2)_{x_{sep}}$: $(\partial^2 p/\partial x^2)_{x_{sep}} = 0$, and $(\partial^2 p/\partial x^2)_{x_{sep}}$ such that $(\partial u/\partial y)_{y=0}$ is continuously zero. Within this field the results would be expected to be roughly correct.

The mathematical method considers these same two values of $\partial^2 p/\partial x^2$ but obtains results which are asymptotically exact as $(x_{sep} - x_0) \to 0$. To each formula it proceeds empirically to add terms of higher order in $(x_{sep} - x_0)$ in order to fit a known precise result at a large value of $(x_{sep} - x_0)$; this then covers the whole range of $(x_{sep} - x_0)$ by interpolation. The two formulae are finally combined by interpolation for $\partial^2 p/\partial x^2$. Since the final formula is thus 'exact' as $(x_{sep} - x_0) \to 0$ and 'correct' for some large value of $(x_{sep} - x_0)$ for each of two values of $\partial^2 p/\partial x^2$, and since the corresponding interpolations are for only second-order effects, the final formula should be reasonably accurate throughout the whole double range. It is afterwards shown that the same formula should hold for all types of pressure distributions that are smooth near separation.

3.1. *The Exact Condition when* $(x_{sep} - x_0) \to 0$.—This section must be started with a semi-physical argument in order to show that for the asymptotic solution only, *i.e.*, as $(x_{sep} - x_0) \to 0$, the initial Blasius velocity profile at $x = x_0$ can be replaced by a straight line profile having the same gradient $\partial u/\partial y$ at the wall.

Given that the pressure gradient $\partial p/\partial x$ is zero for $x < x_0$ and non-zero for $x > x_0$, the point of separation will approach indefinitely close to x_0 as the pressure gradient becomes steeper. In the limit, as $(x_{sep} - x_0) \to 0$, the width of the sub-layer at separation also tends to zero and the point of join between sub-layer and outer layer asymptotes to $y = 0$. Thus within the sub-layer although $\partial u/\partial y$ remains finite all higher non-zero derivatives must become infinite. Consequently for the joining condition it is immaterial to the sub-layer whether the (finite-valued) outer-layer higher derivatives are zero or non-zero, provided the values of $\partial u/\partial y$, and of course u and ψ, are correct. Thus the Blasius and the corresponding straight line profiles are asymptotically equivalent as far as concerns the joining condition between sub-layer and outer layer.

It can further be shown for the two profiles that the outer-layer solutions also are asymptotically the same as $(x_{sep} - x_0) \to 0$; the pressure-gradient forces become infinite so predominating over viscosity, thus the partially inviscid solution of equation (1a) is asymptotically exact, and this gives identical solutions in ψ, u, and $\partial u/\partial y$ for both profiles when $y \to 0$.

Thus it is concluded that for the exact asymptotic solution as $(x_{sep} - x_0) \to 0$ the initial Blasius profile at $x = x_0$ may be replaced by an initial straight line profile with the same gradient $\partial u/\partial y$ at the wall. The problem is therefore reduced to that defined by

$$u \equiv my \text{ for } x < x_0$$

$$\frac{\partial p}{\partial x} \neq 0 \text{ for } x > x_0 .$$

In principle precise solutions of the above are found for the two conditions, $\partial^2 p/\partial x^2 \equiv 0$ for all $x > x_0$ (the corresponding condition in the physical derivation specified $\partial^2 p/\partial x^2 = 0$ only at $x = x_{sep}$) and $\partial^2 p/\partial x^2$ such that $(\partial u/\partial y)_{y=0} \equiv 0$ for all $x > x_0$.

3.1.1. *The solution of $u \equiv my$ for $x < x_0$; $\partial p/\partial x = const$ for $x > x_0$.*

Let
$$g = \frac{1}{\mu}\frac{\partial p}{\partial x}. \qquad \text{(15a)}$$

The transformation:

$$\left.\begin{aligned} \eta &= \frac{gy}{m}; \quad X = \frac{\nu g^3(x - x_0)}{m^4} \\ \bar{u} &= \frac{gu}{m^2}; \quad \bar{v} = \frac{mv}{\nu g}, \text{ and } \frac{\bar{p}}{\frac{1}{2}\bar{u}^2} = \frac{p}{\frac{1}{2}\rho u^2} \end{aligned}\right\} \qquad \text{(15b)}$$

reduces the equations of motion to

$$\left.\begin{aligned} \bar{u}\frac{\partial \bar{u}}{\partial X} + \bar{v}\frac{\partial \bar{u}}{\partial \eta} &= -1 + \frac{\partial^2 \bar{u}}{\partial \eta^2} \\ \frac{\partial \bar{u}}{\partial X} + \frac{\partial \bar{v}}{\partial \eta} &= 0 \end{aligned}\right\} \qquad \text{(16)}$$

with the boundary conditions and the problem represented by

$$\bar{u} \equiv \eta \quad \text{at} \quad X < 0 \qquad \text{(17a)}$$

$$\frac{\partial \bar{p}}{\partial X} \equiv 1 \quad \text{for} \quad X > 0 \qquad \text{(17b)}$$

$$\bar{\psi} = 0 = \bar{u} \text{ at } \quad \eta = 0 \qquad \text{(17c)}$$

$$\frac{\partial \bar{u}}{\partial \eta} \to 1 \quad \text{as} \quad \eta \to \infty \qquad \text{(17d)}$$

[equation (17d) follows *a posteriori* from the differentiated equation of motion:

$$\mu \frac{\partial}{\partial s}\frac{\partial u}{\partial y} = \nu \frac{\partial^3 u}{\partial y^3}\Big]$$

and, from equations (17d) and (16),

$$\frac{\partial^2 \bar{u}}{\partial \eta^2} \to 0 \text{ as } \eta \to \infty \qquad \text{(17e)}$$

$$(\bar{p} + \tfrac{1}{2}\bar{u}^2) = \text{const along a streamline, as } \eta \to \infty . \qquad \text{(17f)}$$

The problem is now non-dimensional and so has some specific numerical solution, say

$$X_{sep} = C \qquad \text{(18)}$$

where C has some definite and specific value.

Substitution of equation (18) into equation (15) gives that the general solution is

$$(p_{sep} - p_0) = \frac{\rho m^4}{g^2} C , \qquad \text{(19)}$$

and further substitution of

$$m = 0\cdot 33206\left(\frac{U_0^3}{\nu x_0}\right)^{1/2} \qquad \text{(20)}$$

which is the value from the Blasius solution[9], gives that the exact asymptotic solution of the original problem when $\partial p/\partial x$ is constant is

$$\left[C_p\left(x_0 \frac{\partial C_p}{\partial x}\right)^2\right] = a ,$$

where
$$a = 8C\,(0\cdot 33206)^4 \ldots \qquad \text{(21)}$$

The exact solution has thus been obtained in principle and it remains only to find the ' once and for all ' value of the constant C. Any of the more accurate standard numerical methods for solving the laminar boundary-layer equations of motion would give this (except that the singularity at $X = 0$ would need special attention) but with limited computational resources it was found for convenience by an extension of the method used in the physical derivation of section 2. The sub-layer velocity profile was expanded up to the tenth power in η (with a correction later for higher powers), not just at separation but at all positions X up to separation, and the joining condition between sub-layer and outer layer then provided an (algebraically involved) differential equation for the skin friction in terms of X. The solution was obtained in the form of a series:

$$\left.\begin{aligned} X = (\bar{p} - \bar{p}_0) &= \frac{\beta}{24}(1 + 3t)(1 - t)^3 [1 + \beta_1 T + \beta_2 T^2 + \ldots] \\ \text{where} \quad t &= \left(\frac{\partial \bar{u}}{\partial \eta}\right)_0 \\ T &= \left(\frac{1}{t} - 1\right) \\ \beta &= 1 \cdot 626 \\ \beta_1 &= 0 \cdot 0562, \qquad \beta_2 = -0 \cdot 0207 \end{aligned}\right\} \quad \ldots \quad (22a)$$

(Since the above is based upon a limited polynomial expansion from the wall used in conjunction with the physical concept of a discreet sub-layer having a definite joining point with the outer layer, Dr. G. E. Gadd has suggested an independent analysis for the flow in the neighbourhood of the singularity at $X = 0$; this analysis agrees well with the above and is presented in Appendix I.)

The series solution was continued numerically working in terms of the square of the skin friction in order to avoid some of the difficulties of the singularity at separation. The solution just before separation was checked satisfactorily for consistency with Goldstein's solution[8] and the actual position of separation was then readily obtained by extrapolation. The result was

$$X_{\text{sep}} = C = 0 \cdot 0784 \pm 4 \text{ per cent.} \quad \ldots \quad (22b)$$

The present lack of precision in equation (22b) results from the limitation on computing resources and is not relevant to the main thesis of the paper; thus for simplicity of presentation and as the principle of the argument is not affected, it will be assumed that the precise value of C is in fact $0 \cdot 0784$. Equation (19) then becomes

$$(p_{\text{sep}} - p_0) = 0 \cdot 0784 \frac{\rho m^4}{g^2} \quad \ldots \quad (23)$$

and equation (21) becomes

$$\left[C_p \left(x_0 \frac{\partial C_p}{\partial x}\right)^2\right] = 7 \cdot 64 \times 10^{-3} . \quad \ldots \quad (24)$$

3.1.2. *The solution of* $u \equiv my$ *for* $x < x_0$; $(\partial u/\partial y)_{y=0} \equiv 0$ *for* $x > x_0$.—Suppose that the pressure distribution is given by

$$p(x) = p(x_0) + \frac{3\rho}{2} K(x - x_0)^{2/3} \text{ for } x > x_0 . \quad \ldots \quad (25)$$

The transformation, similar to the standard $U_1 \propto X^n$ solutions,

$$\left.\begin{aligned} (x - x_0) &= \chi \\ y &= \frac{\nu^{1/2}\chi^{1/3}\xi}{K^{1/4}} \\ \psi &= \chi^{2/3}K^{1/4}\nu^{1/2}S(\xi) \end{aligned}\right\} \quad \ldots \quad (26)$$

reduces the equations of motion to

$$2SS'' - S'^2 = 3(1 - S''') \quad \ldots \quad (27)$$

with the boundary conditions

$$S_0 = 0 = S_0' . \quad \ldots \quad (28)$$

The present analysis is concerned only with $(\partial u/\partial y)_{y=0} = 0$,

i.e.,
$$S_0'' = 0 . \quad \ldots \quad (29)$$

Also, corresponding to equation (17d), the condition away from the wall is

$$S'' \rightarrow \frac{\nu^{1/2}m}{K^{3/4}} = \text{const as } \xi \rightarrow \infty . \quad \ldots \quad (30)$$

The first few terms of the solution in series using equations (27) to (29) only are

$$S = \frac{\xi^3}{3!} - \frac{2}{3}\frac{\xi^7}{7!} + 16\frac{\xi^{11}}{11!} - \frac{16{,}816}{9}\frac{\xi^{15}}{15!} + \ldots . \quad \ldots \quad (31)$$

This can be continued numerically to give

$$S'' \rightarrow \text{const} = 2{\cdot}2292 \text{ as } \xi \rightarrow \infty . \quad \ldots \quad (32)$$

Substitution of equation (32) into the fourth boundary condition, *i.e.*, equation (30), gives that

$$K_{\tau_0 \equiv 0} = \left[\frac{\nu^{1/2}m}{2{\cdot}2292}\right]^{4/3} \quad \ldots \quad (33a)$$

and further substitution for m from equation (20) gives that the required pressure distribution of equation (25) is

$$(p - p_0) = 0{\cdot}23689\,\frac{\rho U_0^2}{2}\left(\frac{x}{x_0} - 1\right)^{2/3}, \quad \ldots \quad (33b)$$

i.e.,
$$C_p = 0{\cdot}23689\left(\frac{x}{x_0} - 1\right)^{2/3} \quad \ldots \quad (33c)$$

this being shown in Fig. 3, curve (a).

This pressure distribution is one of a family; the family provides a set of new exact solutions of the laminar boundary-layer equations when $u \equiv my$ for $x < x_0$, each member having $(\partial u/\partial y)_{y=0} = \text{const}$ for all $x > x_0$.

Appendix II shows that of the above-mentioned family of pressure distributions the one giving flow with continuously zero skin friction has the greatest pressure rise at any station x for given x_0 and m. It seems likely that in practice the corresponding pressure distribution for continuously zero skin friction given initially an ordinary boundary layer attains any given pressure rise in the shortest distance possible, and with the least dissipation of energy, if there is to be neither transition nor boundary-layer control.

Differentiation of equation (33c) shows that it satisfies

$$\left[C_p\left(x_0\frac{\partial C_p}{\partial x}\right)^2\right] = 5{\cdot}91 \times 10^{-3} . \quad \ldots \quad (34)$$

3.2. *Extension to Larger Values of* $(x_{sep} - x_0)$.—3.2.1. *Replacement of* x_0 *by* x_{sep}.—Comparison of equations (13) and (14) with equations (24) and (34) indicates two differences between the results of the physical derivation and those so far from the present section. The difference in the constants is due to the approximation made in the physical derivation for the sub-layer profile shape ; hence the mathematical constants are used and the physical discarded. On the other hand the difference between x_{sep} and x_0 corresponds to an allowance for viscosity in the outer layer between x_{sep} and x_0, as shown by equations (1a) and (1b) (the mathematical method has implicitly neglected this by specifying $u \equiv my$ at $x = x_0$). Hence x_{sep} is incorporated into the mathematical result. The two formulae become

$$\left[C_p \left(x \frac{\partial C_p}{\partial x}\right)^2\right]_{sep} = 7 \cdot 64 \times 10^{-3} \quad \ldots \quad (35)$$

for $\dfrac{\partial p}{\partial x} = \text{const}$,

while for $\tau_0 \equiv 0$,

$$\left[C_p \left(x \frac{\partial C_p}{\partial x}\right)^2\right]_{sep} = 5 \cdot 91 \times 10^{-3} . \quad \ldots \quad (36)$$

The corresponding pressure distribution for $\tau_0 \equiv 0$ becomes

$$C_{p,\,\tau_0 \equiv 0} = 0 \cdot 23689 \left[\log_e\left(\frac{x}{x_0}\right)\right]^{2/3} . \quad \ldots \quad (37)$$

as illustrated in Fig. 3, curve (b).

These formulae are (still) asymptotically exact as $(x_{sep} - x_0)$ tends to zero and they have a larger useful working range in terms of $(x_{sep} - x_0)$; they will now be fitted to exact results at large values of $(x_{sep} - x_0)$.

3.2.2. *Empirical fitting to the exact result of Howarth.*—Substitution of the ' unfitted ' formula into the Howarth pressure distribution gives separation at $\beta x = 0 \cdot 108$ in place of the exact result $\beta x = 0 \cdot 120$. Since the Howarth pressure distribution is an extreme departure from the short sharp pressure gradient for which the formula is asymptotically exact this reasonably close result suggests that the remaining second-order affects of the parameter $(x_{sep} - x_0)$ are small and that an arbitrarily linear interpolation for $(x_{sep} - x_0)/x_{sep}$, arranged to precisely fit the Howarth result, should give reasonable accuracy over the whole range. The formula for $\partial p/\partial x = \text{const}$, i.e., $\partial^2 p/\partial x^2 = 0$, thus becomes

$$\left[C_p \left(x \frac{\partial C_p}{\partial x}\right)^2\right] = 7 \cdot 64 \times 10^{-3} \left(1 + 0 \cdot 35 \frac{x_{sep} - x_0}{x_{sep}}\right) . \quad \ldots \quad (38)$$

(The coefficient $0 \cdot 35$ is much larger than the initial discrepancy as a cube-root operation is involved in finding the pressure rise to separation.)

Actually as the Howarth pressure distribution has a small, but non-zero, value of $\partial^2 p/\partial x^2$, it has to be used indirectly *via* the final formula of the paper in order to obtain the above result for $\partial^2 p/\partial x^2 = 0$. The principle followed however is the same as if the exact result were known beforehand for $\partial^2 p/\partial x^2 = 0$ instead of for the Howarth distribution, and as if this exact result were used directly to extend equation (35) to become equation (38).

3.2.3. *Empirical fitting to Falkner and Skan's exact* X^n *solutions.*—A special case of Falkner and Skan's exact X^n solutions is that giving continuously zero skin friction. At all stages the boundary layer has ' similar ' velocity profiles. The flow with a Blasius profile at $x = x_0$ and zero skin friction continuously thereafter initially has the double profile of sub-layer and outer layer, but eventually the sub-layer spreads throughout and at large values of $(x_{sep} - x_0)$ it must asymptote in shape to the profile of Falkner and Skan's solution. It can be shown that the exact conditions required to give this asymptotic approach will be satisfied if and only if the parameter $(\theta^2/\nu)(\partial U_1/\partial x)$ asymptotes to the Falkner and Skan value, i.e., $-0 \cdot 068$ (Refs. 10 and 5). The modifications required are shown in Figs. 3 and 4, calculation of θ^2 being by means of the Energy Equation[11]. The new pressure distribution can be represented by

$$C_{p,\tau_0 \equiv 0} \equiv 0 \cdot 2369 \left\{ 1 \cdot 013 \log_e \frac{x}{x_0} - 0 \cdot 013 \left(\frac{x}{x_0} - 1 \right) \right\}^{2/3} . \quad .. \quad .. \quad .. \qquad (39)$$

It would again appear that a full range of $(x_{\text{sep}} - x_0)$ can be included without serious error.

Equation (39) and Fig. 3, curve (c) represent the final pressure distribution for continuously zero laminar skin friction; the correspondingly extended separation formula (this time using a linear form in $(x_{\text{sep}} - x_0)/x_0$ instead of in $(x_{\text{sep}} - x_0)/x_{\text{sep}}$ as for equation (38)) becomes:

$$\left[C_p \left(x \frac{\partial C_p}{\partial x} \right)^2 \right]_{\text{sep}} = 5 \cdot 91 \times 10^{-3} \left(1 - 0 \cdot 025 \frac{x_{\text{sep}} - x_0}{x_0} \right) \ldots \quad .. \quad .. \qquad (40)$$

3.3. *Interpolation for General Values of $\partial^2 p/\partial x^2$*.—The formulae

$$\left[C_p \left(x \frac{\partial C_p}{\partial x} \right)^2 \right] = 7 \cdot 64 \times 10^{-3} \left(1 + 0 \cdot 35 \frac{x - x_0}{x} \right) \quad .. \quad .. \qquad (38 \text{ bis})$$

and

$$\left[C_p \left(x \frac{\partial C_p}{\partial x} \right)^2 \right] = 5 \cdot 91 \times 10^{-3} \left(1 - 0 \cdot 025 \frac{x - x_0}{x_0} \right) \quad .. \quad .. \qquad (40 \text{ bis})$$

apply respectively to the pressure distributions represented by $\partial^2 p/\partial x^2 \equiv 0$, and $\partial^2 p/\partial x^2$ such that $\tau_0 \equiv 0$ for $x > x_0$. Suffices $_{\text{sep}}$ are taken as understood.

As the two formulae are closely similar, intermediate types of pressure distribution may be treated by an arbitrarily linear interpolation for $\partial^2 p/\partial x^2$ (although at large values of $(x_{\text{sep}} - x_0)$ the difference becomes rather great to be so bridged). Moreover the resulting formula should be quite reasonably accurate when used as an extrapolation for covering the whole range of $\partial^2 p/\partial x^2$, since it can be shown firstly that $\tau_0 \equiv 0$ gives the maximum possible negative value of $\partial^2 p/\partial x^2$, and secondly that $\partial^2 p/\partial x^2 \equiv 0$ is close to the middle of the range of possible values of $\partial^2 p/\partial x^2$, that is for pressure distributions that are smooth prior to separation. Using this linear interpolation for $\partial^2 p/\partial x^2$ at all stations x, the final result is fitted by

$$\left[C_p \left(x \frac{\partial C_p}{\partial x} \right)^2 \right] = 7 \cdot 64 \times 10^{-3} (1 + 0 \cdot 35 \Delta) \left(1 + 0 \cdot 46 \frac{C_p C_p''}{C_p'^2} \frac{1 + 0 \cdot 14 \Delta}{1 + 0 \cdot 80 \Delta} \right) \quad .. \qquad (41)$$

where Δ, a derived parameter equal to $C_p/\{x(\partial C_p/\partial x)\}$, is introduced as the interpolation parameter in place of $(x_{\text{sep}} - x_0)$, as x_0 would not in practice be well defined. All values in equation (41) refer to conditions at separation, but for the final application x becomes an ' equivalent ' distance, as given later by equation (42).

Equation (41) so far applies to the double parameter (p'', Δ) family of curves sketched in Fig. 5, but the next sub-section shows that it is of general application.

3.4. *Generalization to all Pressure Distributions*.—3.4.1. *Other shapes between x_0 and x_{sep}*.—Even for a given x, C_p, (dC_p/dx) and (d^2C_p/dx^2) at separation, the pressure distribution between x_0 and x_{sep} will still have a range of possible shapes corresponding to a range of values of C_p''', C_p^{IV}, etc., at separation. However since in any case we have, in effect, specified the following conditions, namely that $C_p = 0$ at $x = x_0$, that x, C_p, C_p' and C_p'' are given at separation, and that the curve is a ' smooth ' one (*see* below), the distribution between x_0 and x_{sep} has already been defined within fairly narrow limits and we should not expect any very important effect from the possible variations that remain. On this basis it may be concluded that a pressure distribution of arbitrary shape between x_0 and x_{sep}, whether or not it precisely fitted one of the double parameter family of curves, should still satisfy the final formula (41).

The above assumes a smooth pressure distribution whereas experiments with separated flow sometimes show quite sharp changes of pressure gradient prior to separation, as in Fig. 6. However, the main utilitarian purpose of a formula is to predict whether a given design-pressure distribution will cause separation. Such a pressure distribution would be smooth ; consequently a practical formula does not lose in usefulness by being unable to treat irregular shapes.

3.4.2. *Initial favourable pressure gradients.*—An initial favourable pressure gradient is replaced in the calculation by an equivalent distance with a main stream velocity constant and equal to the peak mainstream velocity in the actual flow. The momentum thickness at x_0 is taken as the criterion of equivalence as this is not affected by the internal readjustment of the profile such as takes place just downstream of x_0 when the actual and the equvalent profiles tend to become of similar shape. Actually the two profiles are likely to be almost identical at x_0 itself, as the momentum thicknesses are thus given equal and, having $\partial p/\partial x = 0$ in both cases (the actual distribution having a pressure peak of x_0), both of the wall derivatives u_0'' and u_0''' are also equal. On the above criterion the Thwaites'[5] or the Energy Equation[11] gives

$$x_0 = \int_0^{x_0'} \left(\frac{U_1}{U_0}\right)^5 dx' \qquad (42)$$

where x is the equivalent distance and x' the actual distance. (A very similar conclusion follows also from the formula of Walz[12] or from that of Young and Winterbottom[13].) With the use of this equivalent distance formula (41) now holds for general types of pressure distribution provided that their form is smooth.

A simpler approximate formula may be taken as

$$\left[C_p \left(x\frac{\partial C_p}{\partial x}\right)^2\right] = 7\cdot 64 \times 10^{-3} , \qquad (43)$$

all values still referring to conditions at separation and x still being the equivalent distance as above.

4. *Discussion.*—4.1. *A Critical Test.*—Hartree[2] has made a precise numerical calculation for the modified pressure distribution from Schubauer's ellipse[14], Fig. 7b. This calculation provides what appears to be the only reliable test data available, experimental work generally allowing too wide a range of interpretation as regards the gradient of pressure $\partial p/\partial x$. With the notation

U_{str} = undisturbed mainstream velocity

U_0 = peak mainstream velocity

x' = distance from actual leading edge

x = distance from the equivalent leading edge

the data can be summarized:

$$U_0^2 = 1\cdot 677 U_{str}^2, \text{ occurring at } x' = 1\cdot 30;$$

at separation

$$U_1^2 = 1\cdot 540 U_{str}^2; \quad x' = 1\cdot 983$$

$$\frac{1}{\frac{1}{2}\rho U_{str}^2}\frac{dp}{dx} = 0\cdot 3516; \quad \frac{1}{\frac{1}{2}\rho U_{str}^2}\frac{d^2p}{dx^2} \simeq +0\cdot 18 .$$

The initial favourable pressure gradient is such that the equivalent distance x as calculated by the Thwaites' or Energy Equation formula of equation (42) is given by

$$x' - x = 1\cdot 30 - 0\cdot 923 = 0\cdot 377 \text{ for } x' > 1\cdot 30 .$$

The above data reduces to

$$C_p = 0 \cdot 0817 \text{ at separation when}$$

$$x = 1 \cdot 606 ; \quad \frac{dC_p}{dx} = 0 \cdot 2095 ; \quad \frac{d^2 C_p}{dx^2} \simeq + 0 \cdot 11 .$$

Thus, for substitution into the formula,

$$x \frac{dC_p}{dx} = 0 \cdot 337 ; \quad \Delta = 0 \cdot 243 ; \quad \frac{C_p C_p''}{C_p'^2} = 0 \cdot 2045 .$$

With these values substituted the formula should give a value for C_p close to the accurate value above of 0·0817. This will now be tested on both the full formula of equation (41) and the approximate formula of equation (43); afterwards are given the positions at which each of these formulae would have predicted separation had the true separation position not been known.

(*a*) The full formula at the true separation position gives

$$C_p = 7 \cdot 64 \times 10^{-3} \frac{(1 \cdot 085)(1 \cdot 0815)}{(0 \cdot 337)^2} = 0 \cdot 0791 .$$

This result is 3·2 per cent low on pressure recovery compared with the true value of 0·0817.

(*b*) The approximate formula at the true separation position gives

$$C_p = \frac{7 \cdot 64 \times 10^{-3}}{(0 \cdot 337)^2} = 0 \cdot 0674 .$$

This result of the approximate version of the formula is 17·5 per cent lower than the true value of the pressure recovery.

(*c*) When the full formula is used to predict the position of separation the error is appreciably less than for the calculations above as C_p, x, and dC_p/dx all increase together. It gives separation to be at $x' = 1 \cdot 976$, instead of at the true position of $x' = 1 \cdot 983$, and then the pressure rise is given by $C_p = 0 \cdot 0802$ which is 2 per cent low.

(*d*) Similarly the approximate formula if used to predict the separation position gives it to be at $x' = 1 \cdot 945$ with the pressure rise 10 per cent low.

Conclusion from the Test.—With errors of only 2 per cent and 3 per cent in the pressure rise to separation the test has provided a confirmation of the final version of the formula. The distance of the separation point from the leading edge—an easier prediction than the pressure rise—is given almost precisely.

The test confirms also the usefulness of the approximate version of the formula in cases where a somewhat larger error is acceptable.

It should be noted that although the agreement in this test could still conceivably be a coincidence, such does not seem likely, as with the method of derivation whereby the formula is based on four exact results with interpolations only for factors of secondary importance, all that would seem required from such a test is to show that no gross factor has been ignored and that the interpolations do behave smoothly as assumed. On this basis, the method of derivation, together with the results of the test, indicate that the formula should give at least quite reasonable accuracy in general cases.

4.2. *Examples*.—In addition to the test of section 4.1 the following will be worked as examples:

(*a*) The Howarth distribution, $U_1 = U_0(1 - \beta x)$.

Since this has been used implicitly in the empirical extension of the formula the exact answer will be expected.

(*b*) The pressure distribution given by $C_p = x/c$.

(*c*) The pressure distributions given by $C_p = (x - x_0)/c$.

(*d*) Also, in connection with the general application of the formula, reference is made to the prediction of laminar boundary-layer shock-wave interaction.

Example (*a*).—The Howarth distribution[1], $U_1 = U_0(1 - \beta x)$.

This distribution has been used in the empirical extension of the formula. It is illustrated in Fig. 7a.

Since $U_1 = U_0(1 - \beta x)$,

$$C_p = 1 - \frac{U_1^2}{U_0^2} = 2\beta x\left(1 - \frac{\beta x}{2}\right),$$

$$\frac{dC_p}{dx} = 2\beta(1 - \beta x) \text{ and} \frac{d^2C_p}{dx^2} = -2\beta^2,$$

$$\Delta = \frac{C_p}{x\frac{dC_p}{dx}} = \frac{1 - \frac{\beta x}{2}}{1 - \beta x}.$$

These algebraic values could be substituted into the formula and the resulting equation solved for the position of separation. Here it is sufficient to verify the result.

At $\beta x = 0{\cdot}120$, which is the exact position of separation as found by Howarth[1] and confirmed by Hartree[15],

$$C_p = 0{\cdot}2256; \qquad x\frac{dC_p}{dx} = 0{\cdot}211$$

$$\Delta = 1{\cdot}067; \qquad C_p' = 1{\cdot}76\beta$$

$$\frac{C_pC_p''}{C_p'^2} = -0{\cdot}1455\,.$$

With these values the formula gives

$$C_p = 7{\cdot}64 \times 10^{-3}\,\frac{(1{\cdot}374)(1 - 0{\cdot}042)}{(0{\cdot}211)^2}$$

$$= 0{\cdot}226 \text{ as required.}$$

Example (*b*).—The pressure distribution given by $C_p = x/c$, or $U_1^2 = U_0^2(1 - x/c)$. This, a special case of Example (*c*), has a constant pressure gradient right from the leading edge. One immediately obtains:

$$C_p = \frac{x}{c}; \qquad C_p' = \frac{1}{c}; \qquad C_p'' = 0$$

$$\Delta = 1{\cdot}0.$$

Hence, at separation

$$\left(\frac{x}{c}\right)^3 = 7{\cdot}64 \times 10^{-3}(1{\cdot}35)(1{\cdot}00)\,.$$

Therefore

$$\left(\frac{x}{c}\right)^3 = 10{\cdot}32 \times 10^{-3}$$

$$C_p = \frac{x}{c} = 0{\cdot}218\,.$$

Example (*c*).—The pressure distributions of Fig. 5b, given by $C_p = (x - x_0)/c$, or $U_1^2 = U_0^2(1 - (x - x_0)/c)$, for $x > x_0$, and $C_p = 0$, or $U_1 = U_0$, for $x < x_0$. This has a constant pressure between $x = 0$ and $x = x_0$ and a constant pressure gradient starting at $x = x_0$. It represents a family of pressure distributions with say x_0/c, $= x_0(dC_p/dx)$, as parameter. It yields:

$$C_p = \frac{x - x_0}{c}; \qquad C_p' = \frac{1}{c}; \qquad C_p'' = 0$$

$$\Delta = \frac{x - x_0}{x}.$$

Hence, at separation

$$\frac{x - x_0}{c}\frac{x^2}{c^2} = 7 \cdot 64 \times 10^{-3}\left(1 + 0 \cdot 35\frac{x - x_0}{x}\right)(1 \cdot 00).$$

For very small C_p the asymptotic behaviour is

$$\frac{x - x_0}{c} = C_p \sim 7 \cdot 64 \times 10^{-3}\left(\frac{c}{x_0}\right)^2;$$

$$\frac{x - x_0}{x_0} \sim 7 \cdot 64 \times 10^{-3}\left(\frac{c}{x_0}\right)^3$$

(and also, by eliminating $\left(\frac{c}{x_0}\right)$,

$$\left(\frac{x - x_0}{x_0}\right)_{\text{sep}} \propto C_{p\,\text{sep}}^{\ 3/2} \text{ (still for small } C_p)\Big).$$

The general result satisfies

$$\frac{x}{c} = 0 \cdot 1970\left[\frac{x}{x - x_0} + 0 \cdot 35\right]^{1/3}$$

and this readily leads to the results given in Table 1 below and Fig. 5b (using $(x - x_0)/x$ as a calculation parameter). This table shows the pressure rise to separation and also the distance to separation as functions of the strength of the adverse pressure gradient.

To solve, for example, the less direct problem of what pressure rise could be obtained at the trailing edge of an aerofoil by a linear pressure gradient starting at mid-chord (with no suction or transition), one has: $x/x_0 = 2 \cdot 0$ and hence $(x - x_0)/x_0 = 1 \cdot 0$, so that the table immediately gives for the conditions at the trailing edge:

$$C_p = 0 \cdot 131, \text{ i.e., } U_1/U_0 = 0 \cdot 932.$$

TABLE 1

$\frac{x_0}{c} = \frac{x_0}{\frac{1}{2}\rho U_0^2}\frac{dp}{dx}$	∞	4·24	0·907	0·386	0·242	0·198	0·131	0·081	0·046	0
$\frac{x_{\text{sep}} - x_0}{x_0}$	0	$1 \cdot 00 \times 10^{-4}$	$1 \cdot 01 \times 10^{-2}$	$\frac{1}{9}$	$\frac{1}{3}$	$\frac{1}{2}$	1	2	4	∞
$C_{p\,\text{sep}}$	0	$4 \cdot 24 \times 10^{-4}$	$0 \cdot 916 \times 10^{-2}$	0·0429	0·0805	0·099	0·131	0·161	0·184	0·218

Example (*d*).—In Ref. 16 the basic physical method, but not the actual formula, is appropriately adapted and used for predicting laminar boundary-layer shock-wave interactions. At least good qualitative agreement is obtained.

4.3. *Some Criticisms.*—A few criticisms of the method are given but these would not appear to detract seriously from its use.

(*a*) The method of treatment of the laminar boundary layer as presented in this paper has been developed for the situation where one requires a prediction concerning separation, and it is not generally suitable for the calculation of the boundary-layer thicknesses such as θ and δ^*. In cases where, having ascertained that separation would not occur, one required to calculate say the momentum thickness θ, as when finding the 'drag' of an aerofoil, the most suitable method is probably that of the Thwaites'[5], or Energy[11] Equation, which gives θ with accuracy and speed. Refs. 12 and 13 (Walz, and Young and Winterbottom) are likewise suitable for calculation of the momentum thickness.

[One valuable exception to the above generalization concerning in particular the displacement thickness δ^* is the prediction of laminar boundary-layer shock-wave interaction. Since at least in the initial stages of this phenomenon the pressure rises are sharp and the values of C_p are small, the basic physical method is valid without the empirical extensions of the full formula, and, as previously mentioned, the author of Ref. 16 has made an appropriate adaptation in order to be able to readily calculate the relation between δ^* and the pressure distribution, in explicit but general terms. This calculation is a necessary step in solving the interaction process between boundary layer and pressure distribution.]

(*b*) If calculating from an experimental pressure distribution the formula requires to a considerable accuracy the value of the pressure gradient $\partial p/\partial x$ at separation. In practice this would require, in a separation region, a steady flow, with accurate readings from closely grouped static tappings; otherwise what at first would appear ample evidence may be found to be capable of a wide interpretation as to the distribution of pressure gradient $\partial p/\partial x$ and hence a very wide interpretation of $(\partial C_p/\partial x)^2$ in the formula; the uncertainty is usually aggravated by the proximity of a point of inflexion in the pressure distribution. This difficulty, however, should not be regarded as a disadvantage of the method; rather, it represents the behaviour of the laminar boundary layer which is highly sensitive to the values of the pressure gradients just in the region of separation (*see* also Ref. 17).

(*c*) Several further calculations would be needed to establish the formula to a higher accuracy. These calculations would include obtaining the coefficient to a higher accuracy, finding a new coefficient to strengthen the extrapolation for positive p'', and working a special case for a third point at an intermediate value of Δ with $p'' = 0$. It is possible also that the higher derivatives at separation, $\partial^3 p/\partial x^3$ and above, that reflect the general shape of the pressure distribution, could be significant, and the argument for neglecting them is in any case only tentative. It does strongly suggest that in general these are not important but in extreme cases the formula should be used with care.

(*d*) In special circumstances the concept of an equivalent x is not always valid. For example, it would not apply to the pressure distribution of Fig. 8a where a sharp pressure fall is immediately followed by a sharp pressure rise. In the limiting case this becomes an 'impulse' of pressure change as in Fig. 8b and this need not affect the boundary layer as a whole whereas the equivalent-distance concept could suggest separation. The concept of an equivalent x should be valid, however, when the favourable pressure gradient occurs sufficiently far upstream for its effect to have distributed itself through the boundary layer before the separation point is reached, and in general this condition would seem likely to hold. In the above connection also there might be some difficulty in deciding, for curves such as that of Fig. 8c, whether the calculation should be on a basis of U_0 at A or U_0 at B; B would be used when the second pressure gradient is relatively steep and occurs some distance downstream of the first, while for large smooth pressure rises after B, either basis should be valid and lead to the same result.

(*e*) It will be found on a closer examination of the algebra of the physical method that, as a result of neglecting the higher terms in the expansion for the Blasius comparison profile, the picture as given is true only for very small pressure rises. *A priori* one does not know even the order of magnitude of the higher terms that must occur in the formula for its application to larger pressure rises, and it is only the empirical extensions which show that these terms are not large and hence are then able to give the formula a valid overall application.

4.4. *Comparison with other Methods*.—As has been mentioned in the Introduction the present method has been developed in order to obtain a simple workable formula and one that gives a clear intuitive understanding. Comparison of its results with those of certain other methods is shown in Table 2 below and in the subsequent Case C. The rapid method of calculation of Von Doenhoff[6] is not quoted in the table but it uses results from calculations by Kármán and Millikan's method of Inner and Outer Solutions.

TABLE 2

Values of the Pressure Rise C_p at Separation as Calculated by Various Methods

(The results are shown also in Fig. 7)

Case A: The pressure distribution of Howarth, $U_1 = U_0(1 - \beta x)$: Fig. 7a.

Case B: The pressure distribution of Hartree: Fig. 7b.

Pressure distribution			Case A	Case B
Exact result[1,2]			$C_p = 0{\cdot}2256$ at $\beta x = 0{\cdot}120$	$C_p = 0{\cdot}0817$
Result by the method of:	Pohlhausen[3]		$C_p = 0{\cdot}287$ at $\beta x = 0{\cdot}156$	not known*
	Kármán and Millikan[4]		$C_p = 0{\cdot}194$ at $\beta x = 0{\cdot}102$	$C_p < 0{\cdot}063$†
	Thwaites[5]		$C_p = 0{\cdot}221$ at $\beta x = 0{\cdot}117$‡	$C_p = 0{\cdot}063$§
	Present paper	Approximate formula	$C_p = 0{\cdot}205$ at $\beta x = 0{\cdot}1085$	$C_p = 0{\cdot}0740$
		Full formula	$C_p = 0{\cdot}226$ at $\beta x = 0{\cdot}120$‡	$C_p = 0{\cdot}0802$‖

* The Pohlhausen result is not known for the Hartree pressure distribution.

† Kármán and Millikan's method gave $C_p = 0{\cdot}063$ (Ref. 17) with approximately Schubauer's original pressure distribution and would therefore be expected to give $C_p < 0{\cdot}063$ for Hartree's pressure distribution, as this has a steeper pressure gradient. (Ref. 18 gives a somewhat larger pressure rise than Ref. 17, the value being sensitive to the pressure gradient in the assumed polynominal pressure distribution.)

‡ Both of these methods use empirical fitting to the Howarth distribution.

§ This is from a calculation on the basis of Ref. 5 but using Hartree's modified pressure distribution in place of Schubauer's.

‖ This is the result of the critical test applied in section 4.1 to the method of the present paper.

Case C: The third pressure distribution is the general one of a steep adverse pressure gradient being applied abruptly at some point say $x = x_0$. According to the methods of, for example, Pohlhausen, Von Doenhoff and Thwaites, a pressure gradient of finite steepness can be sufficient to cause immediate separation with zero pressure rise. The present paper however suggests that some (non-zero) pressure rise must always precede separation unless the pressure gradient is infinitely steep. The only exact solutions known for this case are those derived in sections 3.1.1 and 3.1.2, and in Appendix I of the present paper.

4.4.1. *Comparison with Thwaites' method*.—The method of Thwaites is particularly appropriate for pressure distributions in which the pressure rise to separation is large, whereas the present method, before its empirical extension, is appropriate rather for small pressure rises to separation.

The method of Thwaites uses what can be interpreted as a shape parameter; this shape parameter involves the momentum thickness θ, but, by using a very simple formula for θ, Thwaites makes the method a particularly practicable one.

For obtaining a single result which will apply to all distributions one could extend either of these results to cover the whole range. Extension of the shape-parameter method would meet the complication that, when the pressure rise to separation becomes very small and tends to zero, the value of the shape parameter employed would increase rapidly and tend to infinity. Also it would have the slight disadvantage of working in terms of the indirect variable θ rather than the distance x direct. These factors suggest that it is more suitable to extend the result for small pressure rises to cover all cases, as has been done here, although it is possible that under certain circumstances it would be more appropriate to apply the shape-parameter criterion; in such an event it may be preferable to have a range of values for this parameter and to choose the appropriate one according to the values of the pressure rise and of $\partial^2 p/\partial x^2$, rather than to specify a fixed value as at present is recommended in that method This range of values in place of a single value would closely correspond to the interpolations which make the difference between the full and approximate versions of the formula of the present paper.

The actual parameter used in the method of Thwaites is $(\theta^2/\nu)(\partial U_1/\partial x)$ and, for large pressure rises, and for a given type of pressure distribution (*i.e.*, effectively for a given value of $\partial^2 p/\partial x^2$), this parameter has an almost fixed value at separation. An interesting comparison with this result is that, for very small pressure rises, the present method shows that $C_p^{1/2}(\theta^2/\nu)(\partial U_1/\partial x)$ is fixed at separation.

The above comparison refers only to the calculation of the separation condition; for other calculations the remarks of section 4.3 (*a*) apply.

5. *Conclusion.*—The method of derivation and the satisfactory key check-test suggest that the formula presented in this paper should provide a reasonably accurate solution for laminar boundary-layer separation. The formula is simple and rapid to use and its principle is simple to understand.

During the course of the paper the pressure distribution is derived for continuously zero skin friction, this attaining any given pressure rise in the shortest distance possible for a given laminar boundary layer. A new family of exact solutions is found for the boundary-layer equations of motion, but for rather special conditions in the external flow. These exact solutions are exact solutions for the boundary sub-layer.

The final formula of the paper is given by equation (41); equation (43) is a simpler but rather less accurate formula. The pressure distribution for continuously zero skin friction is represented by equation (39) and is shown in Fig. 3 as curve (c).

Acknowledgments.—The author is indebted to the Staff of the Aeronautics Department for constructive criticism and advice during his term of research at Imperial College, and to the Department of Scientific and Industrial Research for a grant that enabled this research to be undertaken.

LIST OF SYMBOLS

x	Distance around the surface from the (equivalent) leading edge (*see* equation (44))
x'	Distance around the surface from the actual leading edge
x_0	Value of x at the beginning of a sudden adverse pressure gradient
y	Distance from the surface
s	Distance along a streamline
u	Local velocity along a streamline, or local velocity parallel to the surface (these velocities are taken numerically equal in boundary-layer theory)
v	Local velocity perpendicular to the surface
ψ =	$\int_0^y u\,dy$, quantity of flow (per unit spanwise width) between the wall and the point considered
U_{str}	Undisturbed mainstream velocity
U_0	Peak mainstream velocity
U_1	Local mainstream velocity
p	Local static pressure
p_0	Peak suction static pressure, corresponding to U_0
C_p	Pressure coefficient $\frac{p - p_0}{\frac{1}{2}\rho U_0^2} = \left(1 - \frac{U_1^2}{U_0^2}\right)$ = proportion of the peak dynamic head that has been converted to static pressure. The pressure coefficient and its derivatives all take for reference the static pressure and the mainstream dynamic head at the point of peak mainstream velocity, and not conditions at infinity
Δ =	$C_p \Big/ \left(x \frac{\partial C_p}{\partial x}\right)$. This is a parameter behaving like $\frac{x - x_0}{x}$ but used in place of it as x_0 will not in practice be conveniently or well defined.
C_p', C_p'', p', p'', etc.	Partial differentials with respect to x
u', u'', etc.	Partial differentials with respect to y
ρ	Fluid density
μ	Fluid viscosity
ν	Fluid kinematic viscosity $= \frac{\mu}{\rho}$
τ_0	Skin friction $= \mu\left(\frac{\partial u}{\partial y}\right)_0$
m	Parameter $= \left(\frac{\partial u}{\partial y}\right)_0$
θ	Momentum thickness of boundary layer
δ^*	Displacement thickness of boundary layer
δ_s	Value of y at the edge of the sub-layer

$K, g, \bar{u}, \bar{v}, \bar{p}, X, \eta, c, a, t, T, \beta, \beta_1, \beta_2, \chi, \xi, S, h, j$ are sundry quantities used during the algebraic manipulation and defined during the text.

Suffix $_{sep}$ refers to conditions at the position of separation. The whole separation formula and most of its development refers to this position but for convenience the suffix is generally omitted.

Suffix $_b$ refers to the ' Blasius ' or flat-plate comparison flow.

REFERENCES

No.	*Author*	*Title, etc.*
1	S. Goldstein (editor)	*Modern Developments in Fluid Dynamics.* Vol. I, Chapter 4, pp. 173 and 174. (The method of Howarth.) Oxford University Press. 1938.
2	D. R. Hartree	The solution of the equations of the laminar boundary layer for Schubauer's observed pressure distribution for an elliptic cylinder. R. & M. 2427. April, 1939. (*See* also Ref. 15.)
3	S. Goldstein (editor)	As Ref 1 but p. 156 *et seq.* (The method of Pohlhausen.)
4	S. Goldstein (editor)	As Ref. 1 but p. 164 *et seq.* (The method of Kármán and Millikan.)
5	B. Thwaites	Approximate calculation of the laminar boundary layer. *Aero. Quart.*, Vol. I. 1949–50.
6	A. E. Von Doenhoff	A method of rapidly estimating the position of the laminar separation point. N.A.C.A. Tech. Note. 671. 1938.
7	G. E. Gadd..	The numerical integration of the laminar compressible boundary-layer equations, with special reference to the position of separation when the wall is cooled. A.R.C. 15,101. August, 1952.
8	S. Goldstein	On laminar boundary layer flow near a position of separation. *Quart. J. Mech. App. Math.*, Vol. I, p. 43. 1948.
9.	S. Goldstein (editor)	As Ref. 1 but p. 135. (The Blasius solution.)
10	D. R. Hartree	On an equation occurring in Falkner and Skan's approximate treatment of the equation of the boundary layer. *Proc. Camb. Phil. Soc.*, Vol. 33, p. 223. 1937. (Summary in Ref. 1 but p. 140.) *See* also Ref. 5.
11	B. S. Stratford	The energy equation for the incompressible boundary layer. (To be published.) Or *see* Ref. 21.
12	A. Walz	Näherungsverfahren zur Berechnung der laminaren und turbulenten Reibungsschicht. Aerodynamische Versuchsanstalt Göttingen e. V. U. und M. Nr. 3060. 1943.
13	A. D. Young and N. E. Winterbottom.	Note on the effect of compressibility on the profile drag of aerofoils in the absence of shock waves. R.A.E. Report BA.1595. May, 1940.
14	G. B. Schubauer	Air flow in a separating laminar boundary layer. N.A.C.A. Report 527. 1935.
15	D. R. Hartree	A solution of the laminar boundary-layer equation for retarded flow. R. & M. 2426. March, 1939.
16	G. E. Gadd..	On the interaction with a completely laminar boundary layer of a shock wave generated in the mainstream. *J. Ae. Sci.*, Vol. 20, No. 11. November, 1953.
17	C. B. Millikan	A theoretical calculation of the laminar boundary layer around an elliptic cylinder, and its comparison with experiment. *J. Ae. Sci.*, Vol. 3, p. 91. 1936.
18	A. E. von Doenhoff	An application of the von Kármán-Millikan laminar boundary layer theory and comparison with experiment. N.A.C.A. Tech. Note 544. 1935.
19	K. Hiemenz	Gottingen Dissertation, Dingler's Polytech. Journal. (A succession of articles during the year 1911.)
20	A. Fage and V. M. Falkner ..	Further experiments on the flow around a circular cylinder. R. & M. 1369. 1931.
21	E. Truckenbrodt	Ein Quadraturverfahren zur Berechnung der laminaren und turbulenten Reibungsschicht bei ebener und rotationssymmetrischer Strömung. *Ingen. Arch.*, Vol. XX, No. 4, p. 16. 1952.

APPENDIX I

The Solution in the Neighbourhood of the Singularity at $x = x_0$, with Finite Pressure Gradients

By G. E. Gadd, B.A., Ph.D.

With reference to the problem of section 3.1.1, it is possible to obtain an independent solution which fits the boundary-layer equations (but not the full equations of motion) in the neighbourhood of the singularity in the pressure distributions at $x = x_0$. The solution is as follows:

The usual incompressible boundary-layer equation of motion is

$$u\frac{\partial u}{\partial x} + v\frac{\partial u}{\partial y} = -\frac{1}{\rho}\frac{dp}{dx} + \nu\frac{\partial^2 u}{\partial y^2}.$$

Differentiating with respect to y and using the equation of continuity we obtain

$$u\frac{\partial^2 u}{\partial x\,\partial y} + v\frac{\partial^2 u}{\partial y^2} = \nu\frac{\partial^3 u}{\partial y^3}.$$

Suppose the adverse pressure gradient is abruptly applied at $x = x_0$. For x slightly less than x_0, $u = my$ near the wall (*see* section 3.1; m is of course related to x_0), and $\partial^2 u/\partial y^2$ is zero at the wall. Hence putting

$$u = my + u', \qquad r = \frac{\partial u'}{\partial y}$$

and linearizing the equation we obtain for near the wall and x slightly greater than x_0 the relation

$$my\frac{\partial r}{\partial x} = \nu\frac{\partial^2 r}{\partial y^2}.$$

(The linearizations involved can be justified *a posteriori*.)

Put $$r = (x - x_0)^{1/3}R(\eta)\,; \qquad \eta = \left(\frac{m}{3\nu}\right)^{1/3} y(x - x_0)^{-1/3}.$$

The equation becomes $$\eta R - \eta^2 R' = R'' \qquad \ldots \qquad (1)$$

where dashes denote differentiation with respect to η. The boundary condition at the wall, $\mu\frac{\partial^2 u}{\partial y^2} = \frac{dp}{dx}$, becomes

$$R' = \left(\frac{3\nu}{m}\right)^{1/3}\frac{1}{\mu}\frac{dp}{dx}\,; \qquad \eta = 0\,.$$

The solution of equation (1) satisfying this boundary condition can easily be shown to be

$$R = \left(\frac{3\nu}{m}\right)^{1/3}\frac{1}{\mu}\frac{dp}{dx}\eta + AF$$

where A is an arbitrary constant,

and $$F \equiv 1 + \alpha_1\eta^3 + \alpha_2\eta^6 + \ldots + \alpha_m\eta^{3m} + \ldots$$

where
$$\begin{cases} \alpha_1 = \frac{1}{6} \\ \alpha_2 = -\frac{1}{90} \\ \ldots\ldots\ldots\ldots \\ (3m+3)(3m+2)\alpha_{m+1} = -(3m-1)\alpha_m\,. \end{cases}$$

As has been pointed out by Dr. Stuart an alternative relation for F, more suitable for use at large values of η, is

$$F = -\,3^{-4/3}\eta\int_{\infty}^{\eta^3/3} t^{-4/3}\,\mathrm{e}^{-t}\,dt + 3^{-4/3}\eta\int_{\infty}^{0} t^{-4/3}(\mathrm{e}^{-t} - 1)\,dt$$

so that as $\eta \rightarrow \infty$

$$\frac{F}{\eta} \rightarrow 3^{-4/3}\int_{0}^{\infty} t^{-4/3}(1 - \mathrm{e}^{-t})\,dt \equiv G\,.$$

(The approximate value of G is $0{\cdot}94$.)

At large η therefore

$$R' \rightarrow \left(\frac{3\nu}{m}\right)^{1/3}\frac{1}{\mu}\frac{dp}{dx} + AG\,.$$

But
$$R' = \left(\frac{3\nu}{m}\right)^{1/3}\frac{\partial^2 u'}{\partial y^2}\,.$$

Hence R' must $\rightarrow 0$ at large η since, except very near the wall, the fluid must behave as if inviscid, so that the velocity gradient with respect to y remains the same just downstream of x_0 as it was just upstream of x_0. Hence the constant A is finite and determinable; consequently R, u' and u are everywhere finite and determinable.

It is readily shown that the above solution, using the value $G = 0{\cdot}94$, leads to the following asymptotic behaviour at small values of $(x - x_0)$:

$$\left(\frac{\partial u}{\partial y}\right)_0 \sim m - 1{\cdot}536(x - x_0)^{1/3}\frac{1}{\mu}\frac{dp}{dx}\left(\frac{\nu}{m}\right)^{1/3}.$$

The solution given in the text as equation (22a) leads to the same asymptotic form but with $1{\cdot}546$ in place of $1{\cdot}536$.

APPENDIX II

Proof that Continuously Zero Skin Friction Gives the Fastest Possible Pressure Rise when $u \equiv my$ *for* $x < x_0$ *and* $(\partial u/\partial y)_{y=0} = \text{const}$ *for* $x > x_0$

The pressure distributions which give $(\partial u/\partial y)_{y=0} = \text{const}$ for $x > x_0$ when $u \equiv my$ at $x < x_0$ are all contained in the family of exact solutions of section 3.1.2. Equations (25) and (30) show that the fastest possible pressure rise corresponds to the largest possible value of K and hence to the smallest possible value of the limit of S'' as $\xi \rightarrow \infty$. All the members of the family can be represented by appropriate values of S_0'', which corresponds to $(\partial u/\partial y)_{y=0}$, and flow with continuously zero skin friction is represented by $S_0'' = 0$. It is therefore required to show that

$$\left[\frac{\partial}{\partial S_0''}\left(\lim_{\xi\rightarrow\infty} S''\right)\right]_{S_0''=0} = 0\,.$$

Differentiation of equation (27) with respect to some parameter, say ϕ, gives

$$2S\frac{\partial S''}{\partial \phi} + 2S''\frac{\partial S}{\partial \phi} - 2S'\frac{\partial S'}{\partial \phi} = -\,3\frac{\partial S'''}{\partial \phi}\,. \qquad \ldots \quad \ldots \quad \ldots \quad (46)$$

If differentiations with respect to ϕ and ξ can be commuted this becomes

$$2S\frac{\partial^2}{\partial \xi^2}\left[\frac{\partial S}{\partial \phi}\right] + 2S''\left[\frac{\partial S}{\partial \phi}\right] - 2S'\frac{\partial}{\partial \xi}\left[\frac{\partial S}{\partial \phi}\right] = -\,3\frac{\partial^3}{\partial \xi^3}\left[\frac{\partial S}{\partial \phi}\right]. \qquad \ldots \quad \ldots \quad (47)$$

Suppose now that the function S throughout equation (47) is some particular integral, say S^*, of equation (27), i.e., S^* satisfies three specific boundary conditions, and suppose that S^* is known but $[\partial S^*/\partial \phi]$ is not known. Then equation (47) becomes a third-order differential equation for $\partial S^*/\partial \phi$ with known coefficients in terms of S^*, i.e.,

$$2S^* \frac{\partial^2}{\partial \xi^2}\left[\frac{\partial S^*}{\partial \phi}\right] + 2S^{*''}\left[\frac{\partial S^*}{\partial \phi}\right] - 2S^{*'}\frac{\partial}{\partial \xi}\left[\frac{\partial S^*}{\partial \phi}\right] = -3\frac{\partial^3}{\partial \xi^3}\left[\frac{\partial S^*}{\partial \phi}\right] . \quad \ldots \quad \ldots \quad (47a)$$

If, further, there are two such parameters ϕ, say ϕ_1, and ϕ_2, and if these have $\partial S^*/\partial \phi_1 = \partial S^*/\partial \phi_2$ for three independent boundary conditions, then the complete solutions $[\partial S^*/\partial \phi_1]$ and $[\partial S^*/\partial \phi_2]$, which would be obtained from the third-order differential equation (47a), must be identical. Two such parameters are $S_0^{*''}$ and ξ itself; it is assumed that

$$\frac{\partial^2}{\partial \xi \partial S_0^{*''}} = \frac{\partial^2}{\partial S_0^{*''} \partial \xi} \quad \ldots \quad \ldots \quad \ldots \quad \ldots \quad \ldots \quad (48)$$

and then the three boundary conditions are

$$\text{at} \quad \xi = 0 \begin{cases} \dfrac{\partial S^*}{\partial S_0^{*''}} = 0 = \dfrac{\partial S^*}{\partial \xi} = S^{*'} & \ldots \quad (49a) \\[2ex] \dfrac{\partial}{\partial \xi}\dfrac{\partial S^*}{\partial S_0^{*''}} = \dfrac{\partial S^{*'}}{\partial S_0^{*''}} = 0 = \dfrac{\partial}{\partial \xi}\dfrac{\partial S^*}{\partial \xi} = S^{*''} & \ldots \quad (49b) \\[2ex] \dfrac{\partial^2}{\partial \xi^2}\dfrac{\partial S^*}{\partial S_0^{*''}} = \dfrac{\partial S^{*''}}{\partial S_0^{*''}} = 1 = \dfrac{\partial^2}{\partial \xi^2}\dfrac{\partial S^*}{\partial \xi} = S^{*'''} \ldots & \ldots \quad (49c) \end{cases}$$

It therefore follows that

$$\left[\frac{\partial S^*}{\partial S_0^{*''}}\right] \equiv \left[\frac{\partial S^*}{\partial \xi}\right] \quad \ldots \quad \ldots \quad \ldots \quad \ldots \quad \ldots \quad (50)$$

provided S^* is a particular integral of equation (27) satisfying equation (49). [Actually the set (49) represents three independent conditions for equation (47a) but only two for equation (27).] Equation (50) can be verified by expansion in series.

In particular, and again using (48),

$$\lim_{\xi \to \infty}\left[\frac{\partial S^{*''}}{\partial S_0^{*''}}\right] = \lim_{\xi \to \infty}\left[\frac{\partial S^{*''}}{\partial \xi}\right] = \lim_{\xi \to \infty} S''' = 0 . \quad \ldots \quad \ldots \quad \ldots \quad \ldots \quad (51)$$

Again commuting limits (51) becomes

$$\frac{\partial}{\partial S_0^{*''}}\left[\lim_{\xi \to \infty} S^{*''}\right] = 0 . \quad \ldots \quad \ldots \quad \ldots \quad \ldots \quad \ldots \quad (52)$$

This is the result required as (49b) gives that $S^* = [S]_{S_0''=0}$.

The utilitarian significance of this proof probably lies in the indirect support which it gives to the proposition that the quickest possible pressure rise for a given boundary layer whether laminar or turbulent is that with continuously zero skin friction. This proposition in turn suggests that the most efficient type of aerofoil not having external boundary-layer control is, as regards lift/drag ratio, that with laminar flow for the forward portion of the chord, transition, and then zero turbulent skin friction for the remainder of the chord.

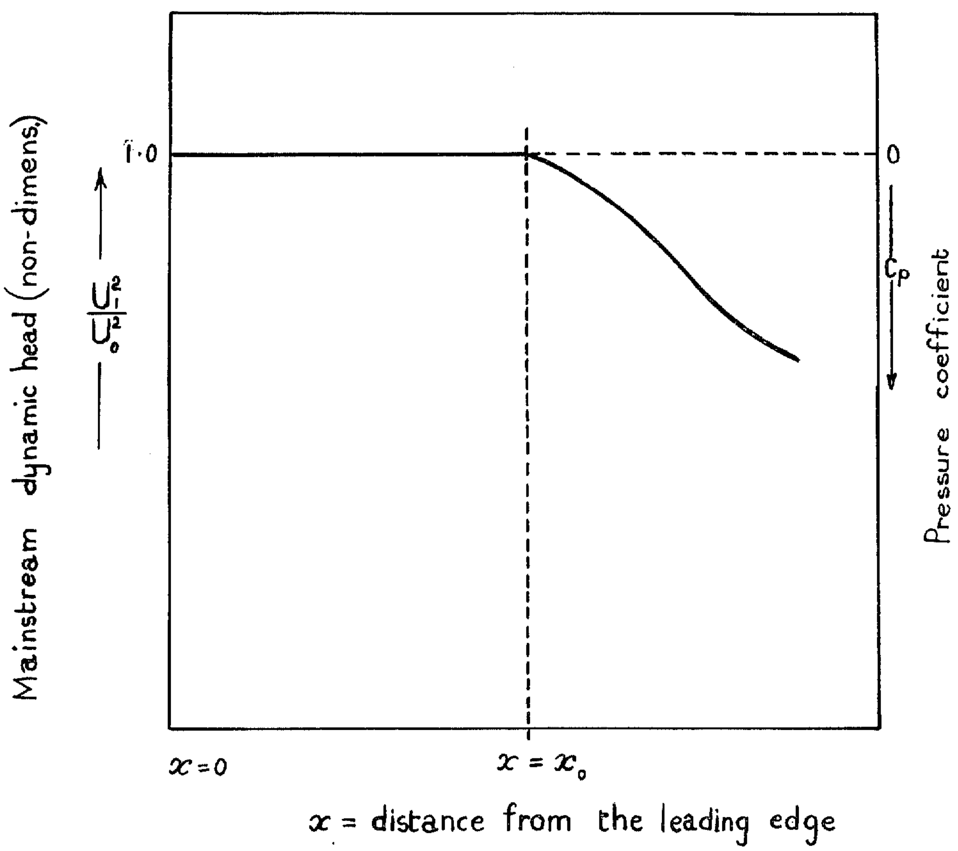

FIG. 1. The type of pressure distribution treated initially by the physical method of derivation

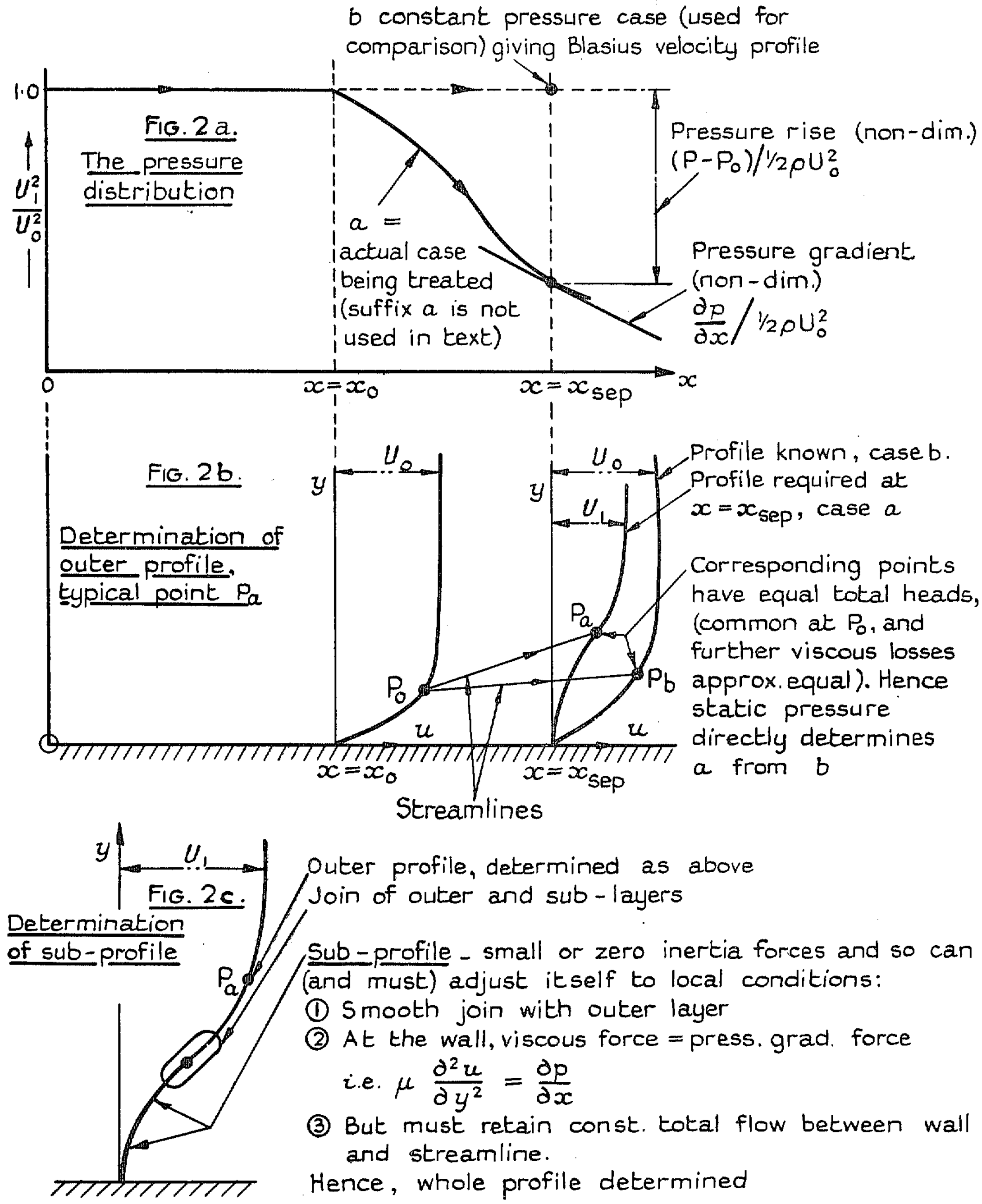

FIGS. 2a to 2c. A simplified representation of the physical method of derivation.

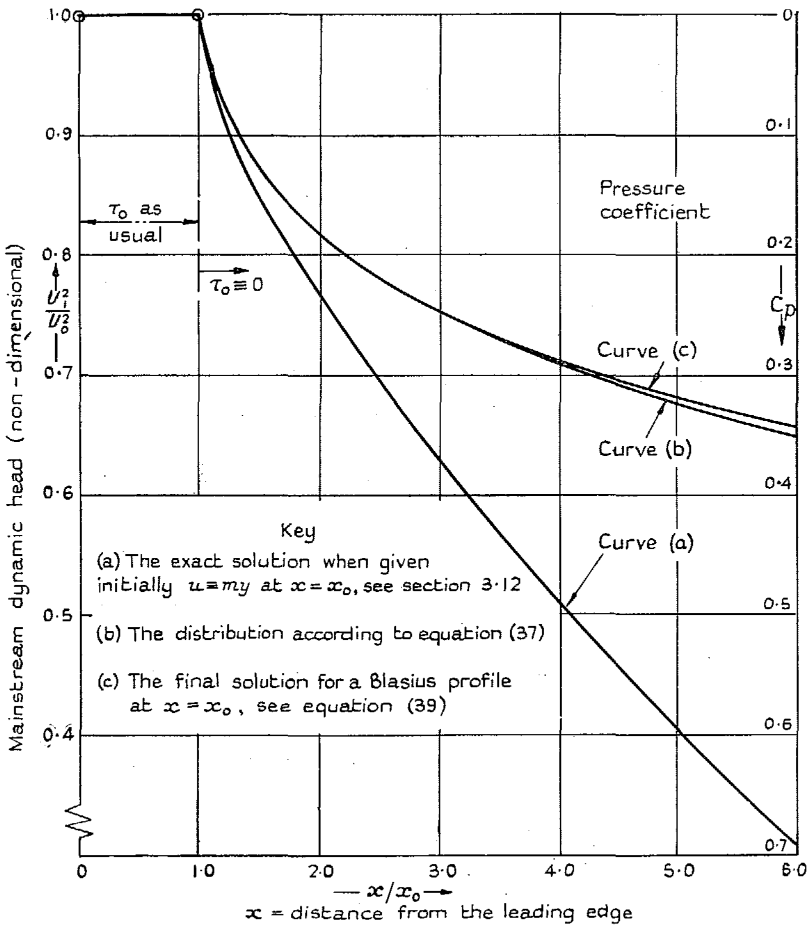

FIG. 3. The pressure distribution for continuously zero skin friction.

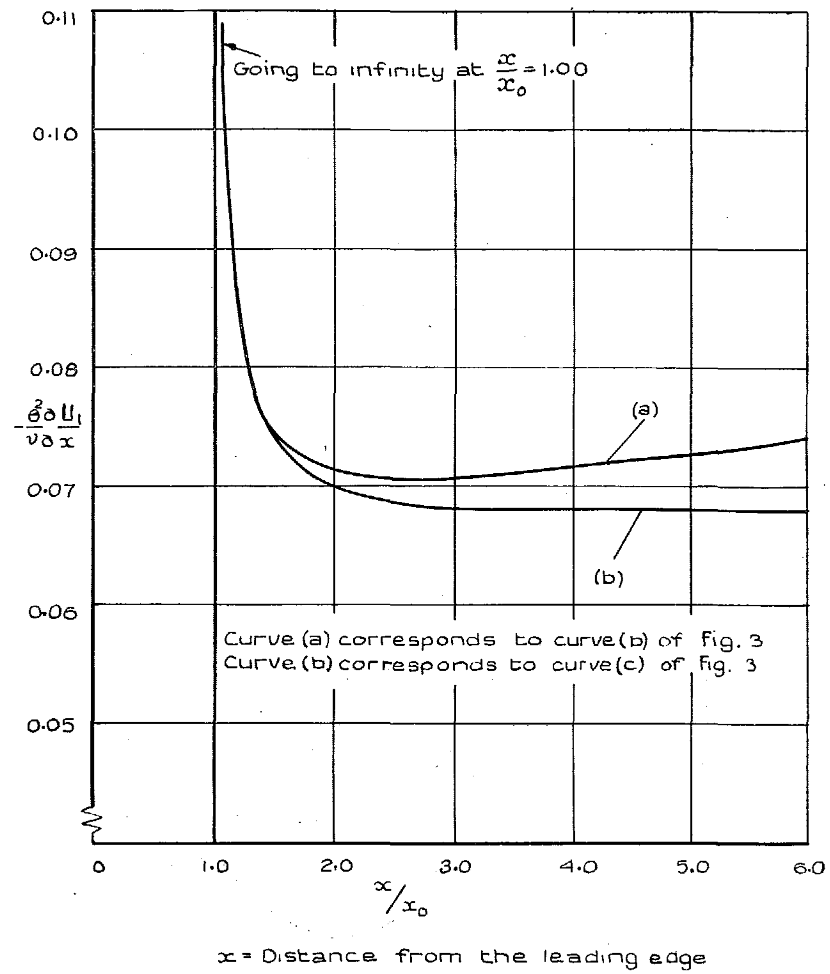

FIG. 4. The value of the parameter $(\theta^2/\nu)(\partial U_1/\partial x)$ for continuously zero skin friction.

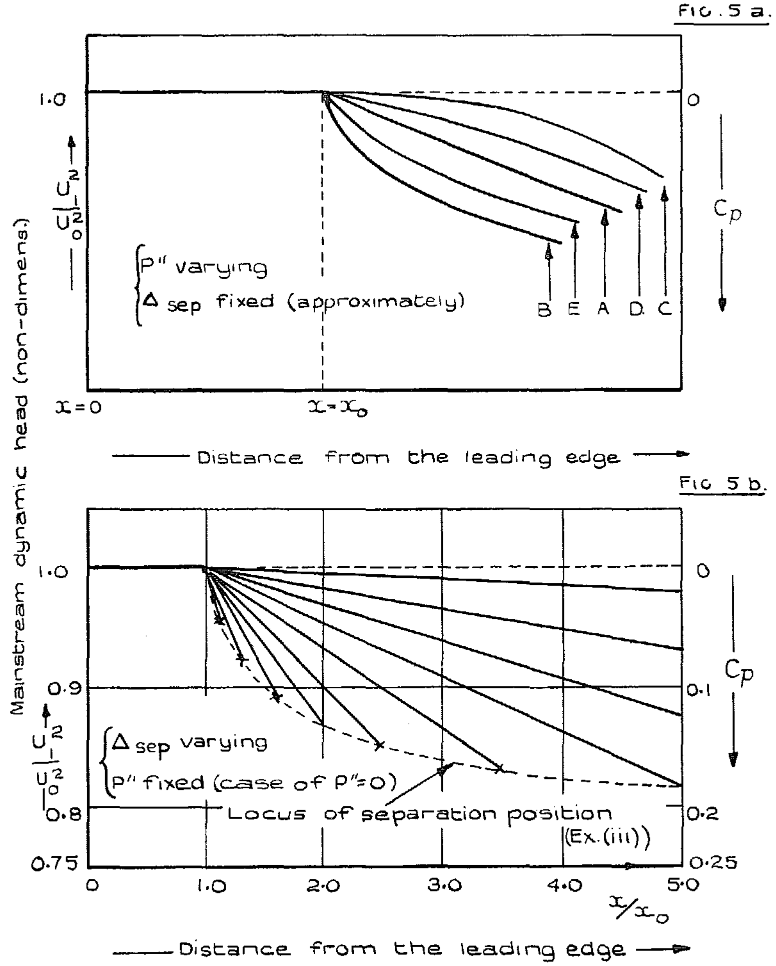

FIGS. 5a and 5b. The (P'', Δ) double parameter family of pressure distributions.

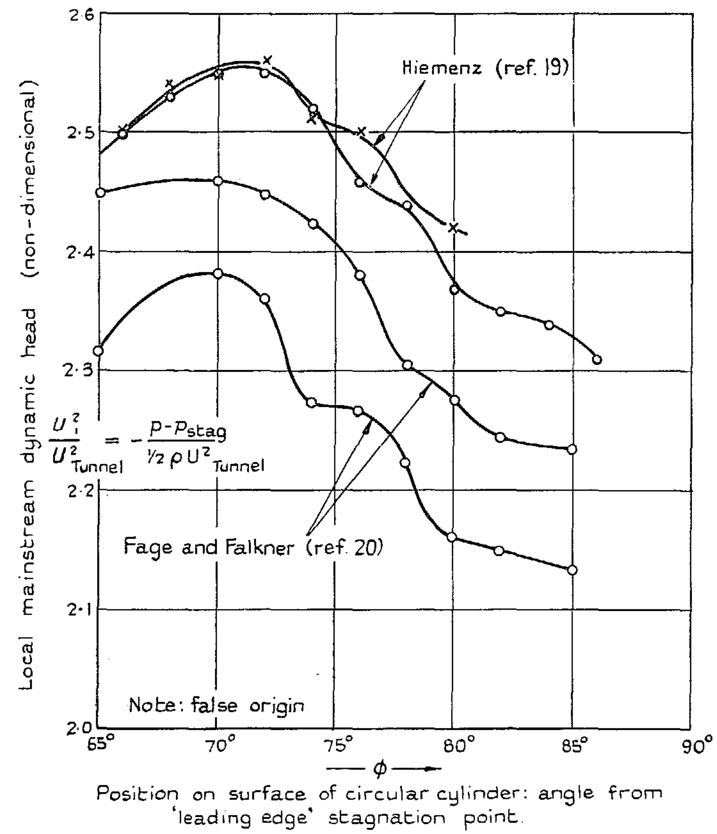

$$\frac{U_1^2}{U^2_{Tunnel}} = -\frac{p - p_{stag}}{\frac{1}{2}\rho U^2_{Tunnel}}$$

FIG. 6. Some experimental pressure distributions in the presence of laminar separation and a wake. Adverse pressure gradient region only. The above are for experiments on circular cylinders ; for an elliptic cylinder *see* Fig. 7.

(5000) Wt. 20/9036 K 7 11/57 Hw.

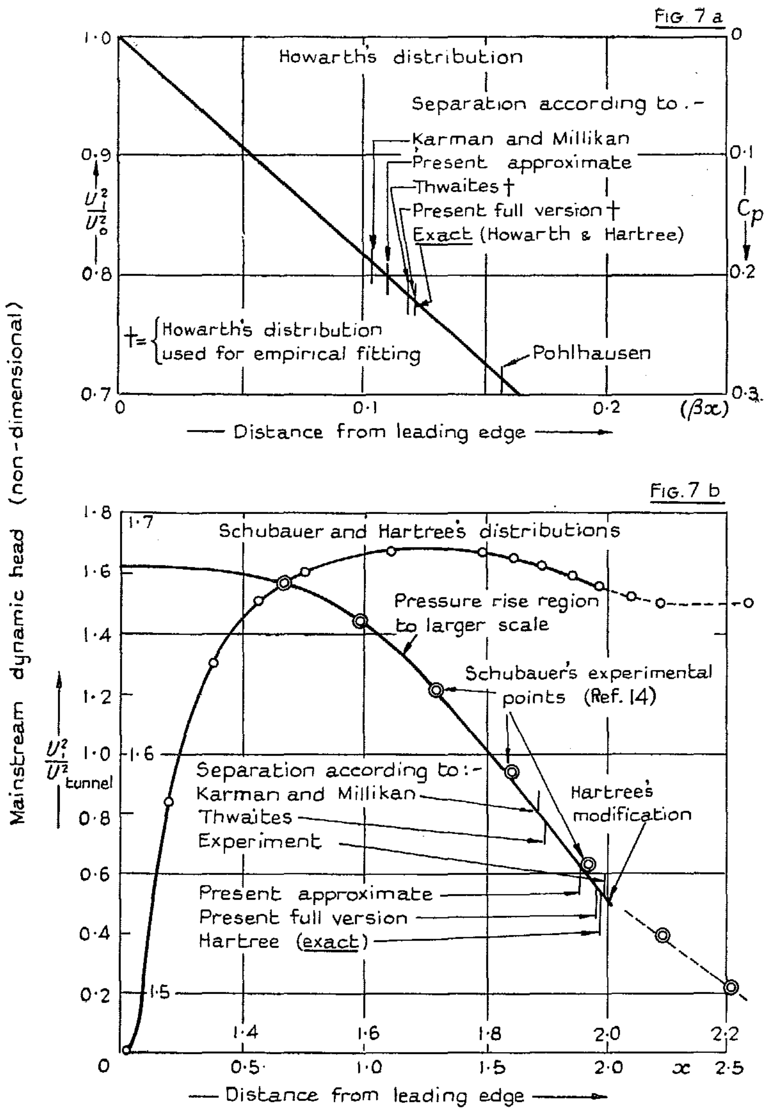

FIGS. 7a and 7b. The pressure distributions for the precise calculations of Hartree and Howarth, and from the experiment of Schubauer.

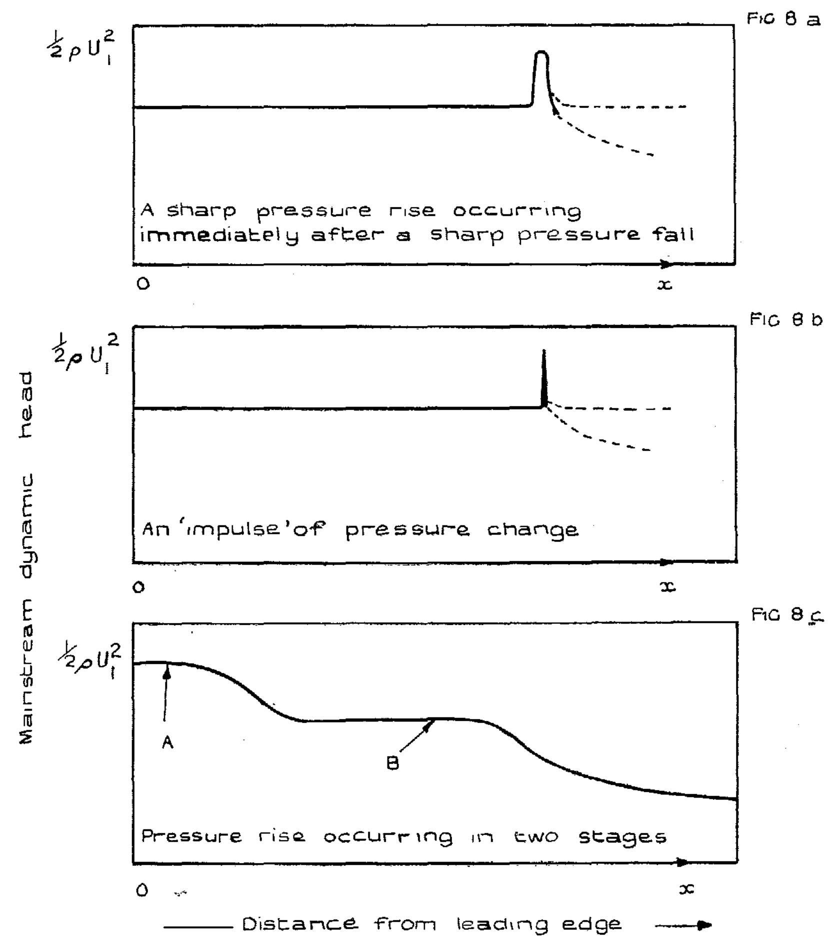

FIGS. 8a to 8c. Some special types of pressure distribution.

Publications of the Aeronautical Research Council

ANNUAL TECHNICAL REPORTS OF THE AERONAUTICAL RESEARCH COUNCIL (BOUND VOLUMES)

1939 Vol. I. Aerodynamics General, Performance, Airscrews, Engines. 50*s.* (51*s.* 9*d.*).
Vol. II. Stability and Control, Flutter and Vibration, Instruments, Structures, Seaplanes, etc. 63*s.* (64*s.* 9*d.*)

1940 Aero and Hydrodynamics, Aerofoils, Airscrews, Engines, Flutter, Icing, Stability and Control Structures, and a miscellaneous section. 50*s.* (51*s.* 9*d.*)

1941 Aero and Hydrodynamics, Aerofoils, Airscrews, Engines, Flutter, Stability and Control Structures. 63*s.* (64*s.* 9*d.*)

1942 Vol. I. Aero and Hydrodynamics, Aerofoils, Airscrews, Engines. 75*s.* (76*s.* 9*d.*)
Vol. II. Noise, Parachutes, Stability and Control, Structures, Vibration, Wind Tunnels. 47*s.* 6*d.* (49*s.* 3*d.*)

1943 Vol. I. Aerodynamics, Aerofoils, Airscrews. 80*s.* (81*s.* 9*d.*)
Vol. II. Engines, Flutter, Materials, Parachutes, Performance, Stability and Control, Structures. 90*s.* (92*s.* 6*d.*)

1944 Vol. I. Aero and Hydrodynamics, Aerofoils, Aircraft, Airscrews, Controls. 84*s.* (86*s.* 3*d.*)
Vol. II. Flutter and Vibration, Materials, Miscellaneous, Navigation, Parachutes, Performance, Plates and Panels, Stability, Structures, Test Equipment, Wind Tunnels. 84*s.* (86*s.* 3*d.*)

1945 Vol. I. Aero and Hydrodynamics, Aerofoils. 130*s.* (132*s.* 6*d.*)
Vol. II. Aircraft, Airscrews, Controls. 130*s.* (132*s.* 6*d.*)
Vol. III. Flutter and Vibration, Instruments, Miscellaneous, Parachutes, Plates and Panels, Propulsion. 130*s.* (132*s.* 3*d.*)
Vol. IV. Stability, Structures, Wind Tunnels, Wind Tunnel Technique. 130*s.* (132*s.* 3*d.*)

Annual Reports of the Aeronautical Research Council—

1937 2*s.* (2*s.* 2*d.*) 1938 1*s.* 6*d.* (1*s.* 8*d.*) 1939–48 3*s.* (3*s.* 3*d.*)

Index to all Reports and Memoranda published in the Annual Technical Reports, and separately—

April, 1950 - - - - R. & M. 2600 2*s.* 6*d.* (2*s.* 8*d.*)

Author Index to all Reports and Memoranda of the Aeronautical Research Council—

1909—January, 1954 R. & M. No. 2570 15*s.* (15*s.* 6*d.*)

Indexes to the Technical Reports of the Aeronautical Research Council—

December 1, 1936—June 30, 1939	R. & M. No. 1850	1*s.* 3*d.* (1*s.* 5*d.*)
July 1, 1939—June 30, 1945	R. & M. No. 1950	1*s.* (1*s.* 2*d.*)
July 1, 1945—June 30, 1946	R. & M. No. 2050	1*s.* (1*s.* 2*d.*)
July 1, 1946—December 31, 1946	R. & M. No. 2150	1*s.* 3*d.* (1*s.* 5*d.*)
January 1, 1947—June 30, 1947	R. & M. No. 2250	1*s.* 3*d.* (1*s.* 5*d.*)

Published Reports and Memoranda of the Aeronautical Research Council—

Between Nos. 2251–2349	R. & M. No. 2350	1*s.* 9*d.* (1*s.* 11*d.*)
Between Nos. 2351–2449	R. & M. No. 2450	2*s.* (2*s.* 2*d.*)
Between Nos. 2451–2549	R. & M. No. 2550	2*s.* 6*d.* (2*s.* 8*d.*)
Between Nos. 2551–2649	R. & M. No. 2650	2*s.* 6*d.* (2*s.* 8*d.*)

Prices in brackets include postage

HER MAJESTY'S STATIONERY OFFICE

York House, Kingsway, London, W.C.2; 423 Oxford Street, London, W.1; 13a Castle Street, Edinburgh 2; 39 King Street, Manchester 2; 2 Edmund Street, Birmingham 3; 109 St. Mary Street, Cardiff; Tower Lane, Bristol 1; 80 Chichester Street, Belfast, *or through any bookseller.*

S.O. Code No. 23-3002